PHYSICAL REVIEW D **80,** 074018 (2009)

Jet energy flow at the LHC

Yoshitaka Hatta and Takahiro Ueda

Graduate School of Pure and Applied Sciences, University of Tsukuba, Tsukuba, Ibaraki 305-8571, Japan

(Received 4 September 2009; published 19 October 2009)

We present a quantitative study of energy flow away from jets by numerically solving the evolution equation derived by Banfi, Marchesini, and Smye, and apply the result to two processes at the LHC: discriminating high-p_t jets originating from decays of heavy electroweak bosons from the QCD background, and the survival probability of the BFKL-initiated dijet rapidity gaps. As a by-product, we find a hidden symmetry of the Banfi, Marchesini, and Smye equation which is a remnant of conformal symmetry.

DOI: 10.1103/PhysRevD.80.074018 PACS numbers: 13.85.Hd, 13.38.Dg

I. INTRODUCTION

As we are entering the era of the Large Hadron Collider (LHC), the importance of jets appears more prominent than ever before. Since many of the signatures of new physics are expected to be observed via hadronic jets in disguise, every bit of information from jet measurements is potentially of great significance and should be carefully analyzed in light of the QCD expectations. (See recent reviews [1,2] and references therein.) However, efforts in this direction often encounter difficulties associated with *energy flow*—the transfer of energy or the transverse momentum away from hard jets due to the multiple emission of soft gluons. The interjet energy flow affects many observables either directly or indirectly, and tends to reduce the precision in their experimental measurements. For instance, a small uncertainty of 1% in the jet energy can lead to a 10% uncertainty in the jet cross section at $p_t \sim 500$ GeV [3].

Normally, the soft radiation responsible for energy flow is encoded in event generators where it is no longer cleanly separable from nonperturbative effects such as the underlying event and hadronization effects. Still, one would like to fully understand at least the perturbative part of the radiation at a quantitative level, and indeed there has been substantial progress in theory along this line over the past decade. Given such progress, it would be very interesting if one could treat energy flow as a useful tool for discovering novel phenomena at the LHC, rather than deeming it a nuisance.

In perturbative QCD, observables related to the interjet energy flow typically involve two hard scales $E \gg E_{\rm out} \gg \Lambda_{\rm QCD}$, where E and $E_{\rm out}$ are the jet and interjet energy scales, respectively. In the weak coupling expansion of such observables, logarithmically enhanced terms of the form $(\alpha_s \ln E/E_{\rm out})^n$ appear due to the miscancellation of real and virtual contributions. These logarithms fall into two classes which are equally important at realistic energies in collider experiments: (i) The *Sudakov* logarithms arise from the direct emission of soft gluons from the primary hard partons (jets), and are thus sensitive to the antenna structure of a given process. They can be exponentiated by a sophisticated resummation procedure [4–6]. (ii) The *nonglobal* logarithms, first pointed out in [7,8], are generated by soft, large-angle emissions from secondary (and ternary, etc.) gluons. These gluons multiply exponentially and form a cascade in the interjet region. One then has to consider the coherent emission of soft gluons from the whole cascade whose structure itself is determined by the previous soft radiation. Because of this complexity, the nonglobal logarithms do not exponentiate, but their resummation required somewhat unconventional strategies.

To date, two equivalent methods to resum the nonglobal logarithms have been proposed. Initially, Dasgupta and Salam developed a Monte Carlo simulation code to actually generate the cascade on a computer [7,8]. This approach was followed by several works where it was primarily used to calculate cross sections which involve rapidity gaps [9–11], as well as to appraise the accuracy of event generators regarding nonglobal observables [12]. Alternatively, Banfi, Marchesini, and Smye (BMS) [13] reduced the problem to solving a nonlinear integro-differential equation. This has paved the way for the remarkable correspondence between the nonglobal logarithms and the Balitsky-Fadin-Kuraev-Lipatov (BFKL) logarithms [14–18].

In this paper we adopt the second approach and perform a detailed study of the BMS equation. We then apply the results to two processes at the LHC where energy flow plays an important role. First, we suggest the possibility of using energy flow as a discriminator of high-p_t jets initiated by highly boosted electroweak bosons from the QCD background. As recently stressed in [19], such jets may result from the decay of TeV-scale new particles, so finding methods to identify them is an urgent task at the dawn of the LHC. Second, we consider the perturbative survival probability of large rapidity gaps created by the BFKL Pomeron exchange. We show how to include the effect of the finite jet cone size in the gap cross section calculated in the BFKL framework. It should be said that in these phenomenological applications, we do not intend to present a complete treatment of the problem. Rather, we shall focus on the perturbatively calculable part of the

process involving energy flow which, with more work, can be successfully interfaced with other details of the collision event.

In Sec. II we briefly review the BMS equation and show that in a certain case it admits a "bonus" symmetry which is essentially a remnant of conformal symmetry. In Sec. III we solve the equation numerically and present the result in various forms that are useful for later purposes. We then devote Secs. IV and V to the applications mentioned above.

II. BMS EQUATION AND ITS HIDDEN SYMMETRY

A. The equation

In [13], Banfi, Marchesini, and Smye proposed a method to quantify the efficiency of energy transfer away from hard jets summing all the single-logarithmic terms in the large-N_c approximation. To explain this, consider back-to-back jets with invariant mass $\sqrt{s} = 2E$ produced in e^+e^- annihilation (Fig. 1). Define the "in" region $\mathcal{C}_{\rm in}$ as a pair of cones with opening angle $\theta_{\rm in}$ pointing to the thrust axes. The complementary region is denoted as $\mathcal{C}_{\rm out}$. Let P be the probability that the total energy (or the total transverse momentum with respect to jets) radiated into $\mathcal{C}_{\rm out}$ is *less* than $E_{\rm out}$

$$\sum_{i\in\mathcal{C}_{\rm out}} E_i \le E_{\rm out}. \tag{1}$$

It has been shown in [13] that P obeys a nonlinear integro-differential equation in the regime $E \gg E_{\rm out}$, provided one generalizes its definition to allow the two jets to point to arbitrary directions $(\Omega_\alpha, \Omega_\beta)$ inside the two cones as in Figs. 2(a) and 2(b). The result is

$$\begin{aligned}\partial_\tau P_\tau(\Omega_\alpha, \Omega_\beta) = &-\int_{\mathcal{C}_{\rm out}} \frac{d^2\Omega_\gamma}{4\pi} \frac{1-\cos\theta_{\alpha\beta}}{(1-\cos\theta_{\alpha\gamma})(1-\cos\theta_{\gamma\beta})} \\ &\times P_\tau(\Omega_\alpha, \Omega_\beta) + \int_{\mathcal{C}_{\rm in}} \frac{d^2\Omega_\gamma}{4\pi} \\ &\times \frac{1-\cos\theta_{\alpha\beta}}{(1-\cos\theta_{\alpha\gamma})(1-\cos\theta_{\gamma\beta})} \\ &\times (P_\tau(\Omega_\alpha, \Omega_\gamma) P_\tau(\Omega_\gamma, \Omega_\beta) \\ &- P_\tau(\Omega_\alpha, \Omega_\beta)),\end{aligned} \tag{2}$$

where the $\theta_{\rm in}$ dependence is implicit and the solid angle integrations are restricted as indicated. The evolution parameter τ reads

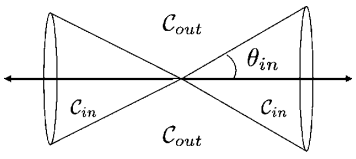

FIG. 1. Back-to-back jets in e^+e^- annihilation.

$$\tau = \bar{\alpha}_s \ln\frac{E}{E_{\rm out}}, \tag{3}$$

in the fixed coupling case ($\bar{\alpha}_s \equiv \alpha_s N_c/\pi$), and

$$\tau = \frac{N_c}{\pi}\frac{1}{2b}\ln\frac{\alpha_s(E_{\rm out})}{\alpha_s(E)} = \frac{N_c}{2\pi b}\ln\left(1 + 2b\alpha_s(E_{\rm out})\ln\frac{E}{E_{\rm out}}\right), \tag{4}$$

with $b = (11N_c - 2n_f)/12\pi$, in the running coupling case. The initial condition is $P_{\tau=0} = 1$ for any points $(\Omega_\alpha, \Omega_\beta)$, and one also has that $P_\tau(\Omega, \Omega) = 1$ for all values of τ (no radiation from a dipole with zero size). The important feature of Eq. (2) is that it resums all the single-logarithmic contributions simultaneously. The Sudakov logarithms are included in the first term on the right-hand side and the nonglobal logarithms in the second, nonlinear term.

As already noted in [13], the equation can be broadly generalized to other hard processes such as hadron-hadron collisions by changing the definition of $\mathcal{C}_{\rm in}$. Namely, the two cones need not be pointing back to back as is relevant to e^+e^- annihilation in the center-of-mass frame, but their relative directions and sizes can be suitably chosen for the process of interest (though this may cause complications when solving the equation numerically). It is even allowed that $\mathcal{C}_{\rm in}$ consists of more than two cones, or only of one cone as in Fig. 2(c). As a matter of fact, we have found that this single-cone configuration is a particularly interesting case both from mathematical and phenomenological points of view, and therefore it will be our main focus in the following.

B. Hidden symmetry

Unfortunately, the nonlinear equation (2) is too complicated to be solved analytically, though a universal feature ("geometric scaling") arises in the large-τ region for which some analytical insights can be given [13]. In realistic collider experiments, there is a rather severe restriction $\tau \lesssim 1 \sim 1.2$, and in this regime the equation has to be studied numerically. Still, here we show that in the single-cone case there exists a hidden symmetry which puts a strong constraint on the solution. For this purpose, it is convenient to employ the exact correspondence [17,18] between the interjet soft gluon cascade and the BFKL dynamics [20,21]. Equation (2) defined on a two-sphere S^2 with the coordinates $\Omega = (\theta, \phi)$ can be mapped onto an equation on a two-dimensional transverse plane $\vec{x} = (x^1, x^2)$ via the stereographic projection (see Fig. 3)

$$x^1 = \tan\frac{\theta}{2}\cos\phi, \qquad x^2 = \tan\frac{\theta}{2}\sin\phi. \tag{5}$$

In the single-cone case, we take the origin of the polar coordinate system in the direction of the cone axis and obtain

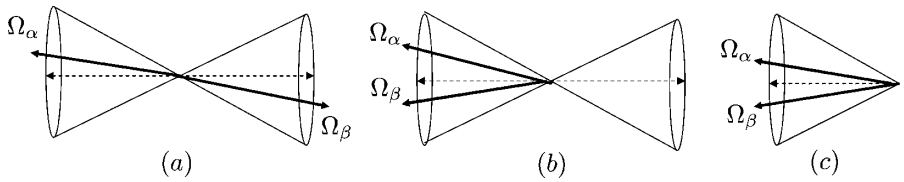

FIG. 2. (a) Two jets in two opposite cones. (b) Two jets in the same cone. (c) The single-cone case. In all configurations the two jets are triggered by a color-singlet $q\bar{q}$ dipole.

$$\partial_\tau P_\tau(\vec{x}_\alpha, \vec{x}_\beta) = -f_{\alpha\beta} P_\tau(\vec{x}_\alpha, \vec{x}_\beta) + \int_{|\vec{x}_\gamma|<r_{\rm in}} \frac{d^2\vec{x}_\gamma}{2\pi} \times \frac{(\vec{x}_\alpha - \vec{x}_\beta)^2}{(\vec{x}_\alpha - \vec{x}_\gamma)^2(\vec{x}_\gamma - \vec{x}_\beta)^2} \times (P_\tau(\vec{x}_\alpha, \vec{x}_\gamma) P_\tau(\vec{x}_\gamma, \vec{x}_\beta) - P_\tau(\vec{x}_\alpha, \vec{x}_\beta)), \tag{6}$$

where

$$f_{\alpha\beta} = \int_{|\vec{x}_\gamma|>r_{\rm in}} \frac{d^2\vec{x}_\gamma}{2\pi} \frac{(\vec{x}_\alpha - \vec{x}_\beta)^2}{(\vec{x}_\alpha - \vec{x}_\gamma)^2(\vec{x}_\gamma - \vec{x}_\beta)^2}. \tag{7}$$

The solid angle integration inside/outside the cone has been mapped onto an integration inside/outside a disk with radius

$$r_{\rm in} = \tan\frac{\theta_{\rm in}}{2}. \tag{8}$$

Let us rescale $\vec{x}/r_{\rm in} \to \vec{x}$ so that $r_{\rm in} = 1$. If one relaxes the restriction $|\vec{x}_\gamma| \le 1$, (6) is identical to the Balitsky-Kovchegov (BK) equation for the dipole S-matrix $S_\tau(\vec{x}_\alpha, \vec{x}_\beta)$, which describes the gluon saturation in high energy scattering [22,23]. As is well known in that context, the integration kernel,

$$\frac{d^2\vec{x}_\gamma}{2\pi} \frac{(\vec{x}_\alpha - \vec{x}_\beta)^2}{(\vec{x}_\alpha - \vec{x}_\gamma)^2(\vec{x}_\gamma - \vec{x}_\beta)^2}, \tag{9}$$

is invariant under conformal transformation which forms the group SL(2, $\mathbb{C}$)

$$z = x^1 + ix^2 \to z' = \frac{\alpha z + \beta}{\gamma z + \delta}, \qquad \alpha\delta - \beta\gamma = 1. \tag{10}$$

Introduction of the boundary $r_{\rm in} = 1$ breaks conformal symmetry down to the subgroup SU(1, 1) $\simeq$ SL(2, $\mathbb{R}$). This maps the interior of the disk onto itself and is defined by the following transformation:

$$z \to z' = \frac{\alpha z + \beta}{\bar{\beta} z + \bar{\alpha}}, \qquad |\alpha|^2 - |\beta|^2 = 1. \tag{11}$$

In the context of the BK equation, conformal symmetry is of limited use because it is broken by the initial condition. However, the initial condition of the BMS equation does have the SU(1,1) symmetry trivially because $P_{\tau=0}(\Omega_\alpha, \Omega_\beta) = 1$ for all $\Omega_{\alpha,\beta}$. A disk which has the isometry group SU(1,1) is known as the Poincaré disk. The invariant measure of the distance (the chordal distance) between two points $(\vec{x}_\alpha, \vec{x}_\beta)$ on the Poincaré disk is (see Appendix A)

$$d^2(\vec{x}_\alpha, \vec{x}_\beta) \equiv \frac{(\vec{x}_\alpha - \vec{x}_\beta)^2}{(1 - \vec{x}_\alpha^2)(1 - \vec{x}_\beta^2)}. \tag{12}$$

Since both the equation and the initial condition are SU(1,1) invariant, the solution $P_\tau(\vec{x}_\alpha, \vec{x}_\beta)$ must also have this symmetry which means that it is a function only of $d^2(\vec{x}_\alpha, \vec{x}_\beta)$ (and τ), or equivalently, only of the geodesic distance

$$l(\vec{x}_\alpha, \vec{x}_\beta) \equiv \cosh^{-1}(1 + 2d^2(\vec{x}_\alpha, \vec{x}_\beta)) = 2\cosh^{-1}\sqrt{1 + d^2(\vec{x}_\alpha, \vec{x}_\beta)}. \tag{13}$$

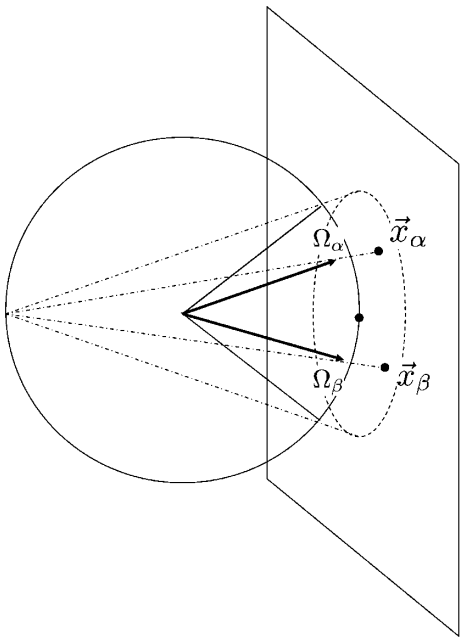

FIG. 3. Stereographic map between a sphere with unit diameter and a plane. The angles (θ, ϕ) are measured with respect to the cone axis.

In order to demonstrate the usefulness of this observation, consider the integral (7). This can be easily evaluated if one sets $\vec{x}_\beta = \vec{0}$. The result is, restoring $r_{\rm in}$,

$$f_{\alpha 0} = \frac{1}{2}\ln\frac{1}{1-\frac{\vec{x}_\alpha^2}{r_{\rm in}^2}}. \tag{14}$$

Using the relation

$$d^2(\vec{x}_\alpha, \vec{0}) = \frac{\vec{x}_\alpha^2}{r_{\rm in}^2 - \vec{x}_\alpha^2}, \tag{15}$$

one can write

$$f_{\alpha 0} = \tfrac{1}{2}\ln(1 + d^2(\vec{x}_\alpha, \vec{0})). \tag{16}$$

Since $f_{\alpha\beta}$ is a function only of $d^2(\vec{x}_\alpha, \vec{x}_\beta)$, the result with generic $\vec{x}_\beta \neq \vec{0}$ is simply given by

$$\begin{aligned} f_{\alpha\beta} &= \frac{1}{2}\ln(1 + d^2(\vec{x}_\alpha, \vec{x}_\beta)) \\ &= \frac{1}{2}\ln\left(1 + \frac{r_{\rm in}^2(\vec{x}_\alpha - \vec{x}_\beta)^2}{(r_{\rm in}^2 - \vec{x}_\alpha^2)(r_{\rm in}^2 - \vec{x}_\beta^2)}\right) \\ &= \frac{1}{2}\ln\left(1 + \frac{\sin^2\theta_{\rm in}(1-\cos\theta_{\alpha\beta})}{2(\cos\theta_\alpha - \cos\theta_{\rm in})(\cos\theta_\beta - \cos\theta_{\rm in})}\right), \end{aligned} \tag{17}$$

where in the second line we switched back to the original sphere problem using the stereographic projection. It requires a considerable amount of work if one tries to get the same result for $f_{\alpha\beta}$ by directly evaluating the integral (7) with $\vec{x}_\beta \neq 0$.

Similarly, the full solution $P_\tau(\vec{x}_\alpha, \vec{x}_\beta)$ can be obtained from $P_\tau(\vec{x}_\alpha, \vec{0})$ which is a function only of $|\vec{x}_\alpha|/r_{\rm in}$

$$P_\tau(\vec{x}_\alpha, \vec{0}) \equiv P_\tau\left(\frac{|\vec{x}_\alpha|}{r_{\rm in}}\right) = P_\tau\left(\sqrt{\frac{d^2(\vec{x}_\alpha, \vec{0})}{1 + d^2(\vec{x}_\alpha, \vec{0})}}\right). \tag{18}$$

$P_\tau(\vec{x}_\alpha, \vec{x}_\beta)$ for generic $\vec{x}_\beta \neq \vec{0}$ is given by

$$P_\tau(\vec{x}_\alpha, \vec{x}_\beta) = P_\tau\left(\sqrt{\frac{d^2(\vec{x}_\alpha, \vec{x}_\beta)}{1 + d^2(\vec{x}_\alpha, \vec{x}_\beta)}}\right) = P_\tau\left(\frac{|z_\alpha - z_\beta|}{|1 - z_\alpha \bar{z}_\beta|}\right). \tag{19}$$

In practice, when solving (6) [or (2)] numerically, one registers the values of P_τ for all (discretized) points $(\vec{x}_\alpha, \vec{x}_\beta)$ at each step of iteration. This can be done straightforwardly without really caring about the constraint (19). The advantage of (19) is that a single plot of the function $P_\tau(\vec{x}_\alpha, \vec{0})$ thus obtained tells the value of P_τ for an arbitrary point $(\vec{x}_\alpha, \vec{x}_\beta)$.

Going back to the sphere problem, (18) implies that

$$P_\tau(\Omega, 0) = P_\tau\left(\frac{\tan\frac{\theta}{2}}{\tan\frac{\theta_{\rm in}}{2}}\right) = P_\tau(e^{\eta_{\rm in} - \eta}), \tag{20}$$

where the pseudorapidity variable η is defined as usual

$$\eta = \ln\cot\frac{\theta}{2}. \tag{21}$$

Equation (20) shows that, if one of the jets is along the cone axis, P becomes a function only of the relative rapidity between the other jet and the cone edge. This is of course a consequence of boost invariance. In the $\vec{x}$ coordinate, it has a very simple meaning as the dilatation symmetry $\vec{x} \to c\vec{x}$. Once the cone size is fixed, the boost invariance is lost, and naively one would expect that the only symmetry of the solution $P_\tau(\Omega_\alpha, \Omega_\beta)$ would be the trivial ϕ rotation. Remarkably, however, a part of conformal symmetry of the soft emission probability survives, and this reduces the 4 degrees of freedom $(\Omega_\alpha, \Omega_\beta)$ to 1. Note that the SU(1,1) symmetry no longer exists if there are two cones forming $\mathcal{C}_{\rm in}$. However, we shall see that the difference in the numerical solutions with and without the backward cone turns out to be quite small.

III. NUMERICAL RESULTS

In this section we present the numerical solution of Eq. (2) extending the initial result in [13]. In doing so, it is useful to factor out the Sudakov contribution

$$P_\tau(\Omega_\alpha, \Omega_\beta) = e^{-\tau f_{\alpha\beta}} g_\tau(\Omega_\alpha, \Omega_\beta), \tag{22}$$

where $f_{\alpha\beta}$ is given by (17) in the single-cone case [Fig. 2(c)], and by Eq. (C.1) of [13] in the case where two cones are pointing back to back [Figs. 2(a) and 2(b)]. The effect of the nonglobal logarithms is then contained in g_τ. At small $\tau \ll 1$, only the Sudakov contribution is important, whereas at large $\tau \gg 1$ the nonglobal contribution dominates in the sense that $e^{-\tau f} \gg g_\tau$. In the phenomenologically relevant range $\tau \sim 1$, the two contributions are comparable. Note that in the single-cone case, f and g_τ are separately SU(1,1) symmetric.

Let us first consider the two-cone case. We fix $\theta_\beta = 0$, $\theta_{\rm in} = \pi/3$ and plot $P_\tau(\theta_\alpha \equiv \theta, 0)$ for four values of τ between 0.6 and 1.2 in Fig. 4. The dotted curves denote the Sudakov contribution alone. The result shows the expected behavior; for small θ corresponding to a dipole (dijet) with small opening angle, energy flow is suppressed due to the QCD coherence and P is close to 1. On the other hand, P is significantly less than 1 for dijets forming a large angle $\theta > 2\pi/3$. One also sees that the nonglobal contribution becomes more important as τ gets larger.

Next, we consider the single-cone case and show in Fig. 5 the "master function" (20) in the same range $0.6 \leq \tau \leq 1.2$ as a function of $\frac{\tan\theta/2}{\tan\theta_{\rm in}/2}$ (left panel) and of $\eta - \eta_{\rm in}$ (right panel). Again the dotted curves represent the Sudakov factor which in this case reads

$$e^{-\tau f} = \left(1 - \frac{\tan^2\frac{\theta}{2}}{\tan^2\frac{\theta_{\rm in}}{2}}\right)^{\tau/2}. \tag{23}$$

In fact, numerically the result in Fig. 5 is very close to the

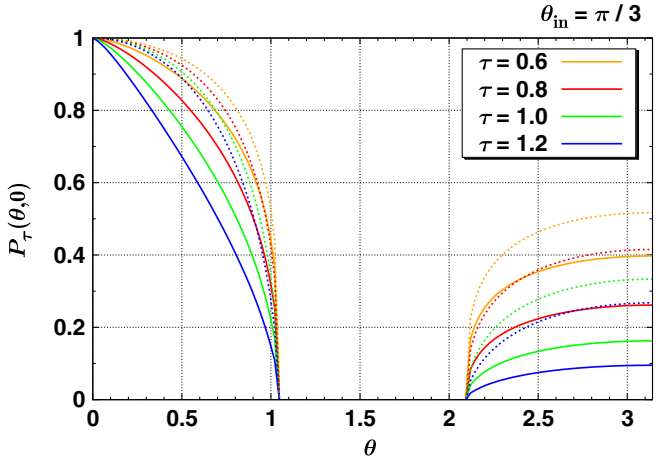

FIG. 4 (color online). Solid curves: the numerical solution of Eq. (2) in the two-cone case. Dotted curves: the Sudakov contribution. Four curves correspond to different values of τ: From top to bottom, $\tau = 0.6$, 0.8.1.0, and 1.2.

left branch of Fig. 4; that is, the difference between Figs. 2(b) and 2(c) is tiny, less than 1% even for θ_{in} as large as $\pi/3$. This means that when the two jets are in the same cone the effect of the backward cone is negligible, and practically one has the SU(1,1) symmetry to a very good approximation.

Finally, we consider the probability that the interjet energy fraction

$$e \equiv \frac{1}{E}\sum_{i\in\mathcal{C}_{out}} E_i \tag{24}$$

is exactly $e_{out} \equiv E_{out}/E$. This may be obtained by differentiating P_τ with respect to E_{out}. For simplicity, we work in the fixed coupling case and denote the distribution of e_{out} as $W(e_{out})$. By definition,

$$\int_0^{e_{out}} W(e)de = P_\tau, \tag{25}$$

or equivalently,

$$W(e_{out}) = \frac{\partial}{\partial e_{out}} P_\tau = -\bar{\alpha}_s e^{\tau/\bar{\alpha}_s}\frac{\partial P_\tau}{\partial \tau}. \tag{26}$$

The function $W(e_{out})$ with $\bar{\alpha}_s = 0.17$ is plotted in Fig. 6 for the back-to-back case (left panel) and the single-cone case (right panel); the latter is obtained from (20) with a particular value $\tan\frac{\theta}{2}/\tan\frac{\theta_{in}}{2} = 0.46$ to be relevant later. W is sharply peaked in the small-e_{out} region ($e_{out} \ll \alpha_s$) where the soft approximation is reliable, and the suppression in the "large"-e_{out} region ($e_{out} \sim \alpha_s$) is stronger in the single-cone case as expected from the coherence effect. Though not shown in the figure, W actually starts to decrease as e_{out} becomes extremely small ($e_{out} < 10^{-5}$). This can be understood from the asymptotic large-τ analysis in [8,13].

Figure 6 shows that in the majority of events the interjet energy flow is very small $E_{out} \ll \alpha_s E$. These typical events do not contribute to the *average* of E_{out} which is dominated by rare events with $E_{out} \gtrsim \alpha_s E$. Indeed, in the present context it is tempting to define the average of E_{out} as

$$\langle e_{out}\rangle = \int_0^1 de_{out} W(e_{out}) e_{out} = -\int_0^\infty d\tau e^{-(\tau/\bar{\alpha}_s)}\frac{\partial P_\tau}{\partial \tau}$$
$$= 1 - \frac{1}{\bar{\alpha}_s}\int_0^\infty d\tau e^{-\tau/\bar{\alpha}_s} P_\tau, \tag{27}$$

where in the last equality we have integrated by parts. Clearly, the integral is dominated by the region $\tau \lesssim \bar{\alpha}_s$ corresponding to $E > E_{out} \gtrsim \alpha_s E$. The soft approximation is not reliable for such large values of E_{out}; one has to use instead the full splitting function to compute $\langle E_{out}\rangle$ (see, e.g., [24]). Thus, although the probability distribution $W(e_{out})$ is meaningful at small $e_{out} \ll 1$, it is not entirely legitimate to compute the average of e_{out} using (27). Nevertheless, the calculation is simple enough and can be

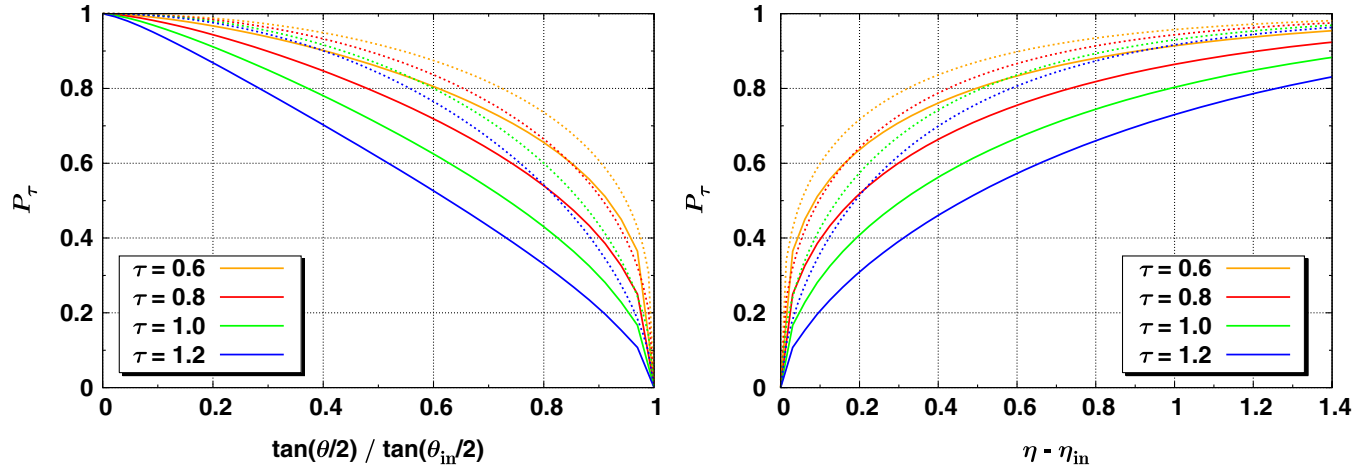

FIG. 5 (color online). Numerical solution of Eq. (2) in the single-cone case.

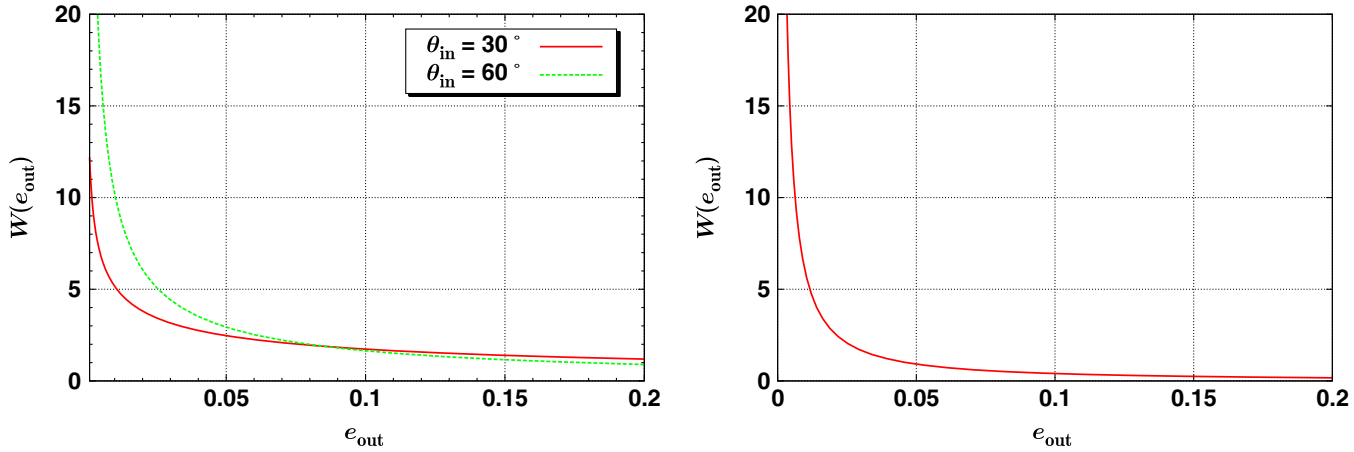

FIG. 6 (color online). The probability distribution of interjet energy fraction $W(e_{\rm out})$. Left panel: Two-cone case with back-to-back jets. Right panel: Single-cone case.

done analytically since it is dominated by the Sudakov contribution. Moreover, the result may be useful to infer the qualitative feature of the differential spectrum of $E_{\rm out}$ in the interjet region. We outline such calculations in Appendix B.

Having discussed the detailed properties of the probability distribution P_τ, we now turn to its phenomenological applications in collider experiments.

IV. HIGH-p_t JETS FROM HEAVY ELECTROWEAK BOSONS

At the LHC, highly boosted heavy electroweak bosons (W, Z, Higgs) can serve as a signal of new physics. For example, they arise as decay products of TeV-scale new particles in certain extensions of the standard model (see [19], and references therein). In order to maximize the potential of discovery, clearly it is desirable to be able to identify these events in hadronic (as well as leptonic) decay channels. Then the issue arises as to how one can experimentally distinguish, preferably event by event, massive jets originating from boosted weak bosons (signal) from QCD jets in the same mass range (background) initiated by light quarks and gluons [25,26]. Reference [26] looked into the substructure of jets for this purpose and showed that it has different characteristic behaviors depending on the progenitor. (For related works, see [27–31].) Somewhat complementary to this, here we investigate the pattern of energy flow outside the jet cone as a possible discriminator of weak boson/QCD jets. Our goal in this section is not to make a practical proposal that is readily useful in experiments, but rather to give the first quantitative study of the difference in energy flow between the two types of jets which will lay the foundation for future work.

Figure 7 shows a "two-pronged" jet at midrapidity originating from a high-p_t boson (say, Z^0) of mass $M \ll p_t$ together with those from a quark with virtuality M. The opening angle between the two primary decay particles inside the jet is bounded from below

$$\theta_{\alpha\beta} \gtrsim 2\frac{M}{p_t}, \tag{28}$$

in both cases, with the lower bound $\theta_{\alpha\beta} \sim 2M/p_t$ being the most probable configuration. Away from this peak, the

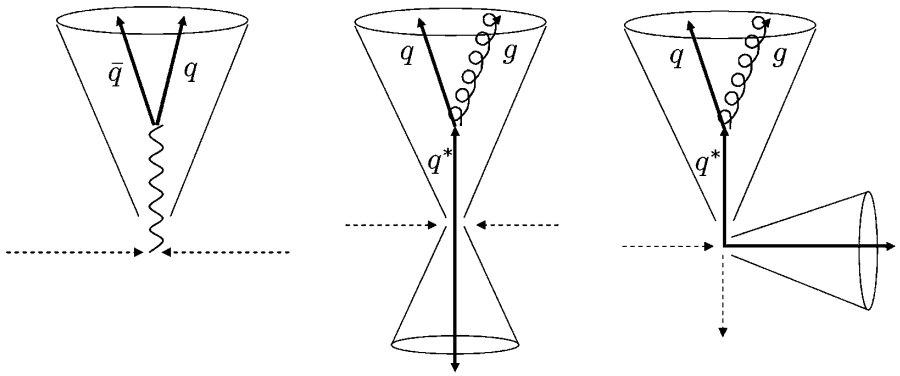

FIG. 7. Left: Massive weak boson jet at midrapidity. Middle and right: Massive quark jet together with an accompanying jet ("color neutralizer").

two types of jets have different particle distributions in $\theta_{\alpha\beta}$ [26].

In the case of a weak boson jet, radiation from the (color-singlet) $q\bar{q}$ pair is strongly suppressed due to the QCD coherence. Let us quantify this statement by computing the probability P_τ discussed in the previous section. We assume that the jet is produced around midrapidity $\eta \approx 0$ and the $q\bar{q}$ pair is symmetrically emitted so that $\Omega_\alpha = (\theta, 0)$, $\Omega_\beta = (\theta, \pi)$ with $\tan\theta = M/p_t$, where the polar angles are measured with respect to the triggered jet axis. We then identify the jet cone with $\mathcal{C}_{\rm in}$ (i.e., the single-cone case) by taking $\theta_{\rm in} \approx R$ where $R = \sqrt{\Delta\eta^2 + \Delta\phi^2}$ is the usual jet cone radius. (Around midrapidity, $\Delta\theta \approx \Delta\eta$ for small $R = \Delta\eta$.) Using the SU(1,1) symmetry (19), one can show that the configuration $\Omega_\alpha = (\theta, 0)$, $\Omega_\beta = (\theta, \pi)$ is equivalent to the configuration

$$\Omega'_\alpha = (\theta', 0), \qquad \Omega'_\beta = (0, 0), \tag{29}$$

where θ' satisfies

$$\frac{\tan\frac{\theta'}{2}}{\tan\frac{R}{2}} = \frac{2\frac{\tan(\theta/2)}{\tan(R/2)}}{1 + \frac{\tan^2(\theta/2)}{\tan^2(R/2)}}. \tag{30}$$

This means that

$$P_\tau(\Omega_\alpha, \Omega_\beta) = P_\tau\left(\frac{2\frac{\tan(\theta/2)}{\tan(R/2)}}{1 + \frac{\tan^2(\theta/2)}{\tan^2(R/2)}}\right), \tag{31}$$

namely, the probability distribution can be obtained from the master function $P_\tau(x)$ merely by the change of variables. We take $E = p_t = 1$ TeV and $E_{\rm out} = 10$ GeV with $\alpha_s(E_{\rm out}) \approx 0.18$ in (4) to get $\tau \approx 0.6$. In Fig. 8, we have plotted $P_{\tau=0.6}$ as a function of

$$\frac{\tan\frac{R}{2}}{\tan\frac{\theta}{2}} \approx \frac{p_t R}{M}. \tag{32}$$

The upper curve is the Sudakov contribution which in this case reads [cf. (23) and (30)]

$$\left(1 - \left(\frac{2\frac{\tan(\theta/2)}{\tan(R/2)}}{1 + \frac{\tan^2(\theta/2)}{\tan^2(R/2)}}\right)^2\right)^{\tau/2} = \left(\frac{\frac{\tan^2(R/2)}{\tan^2(\theta/2)} - 1}{\frac{\tan^2(R/2)}{\tan^2(\theta/2)} + 1}\right)^\tau. \tag{33}$$

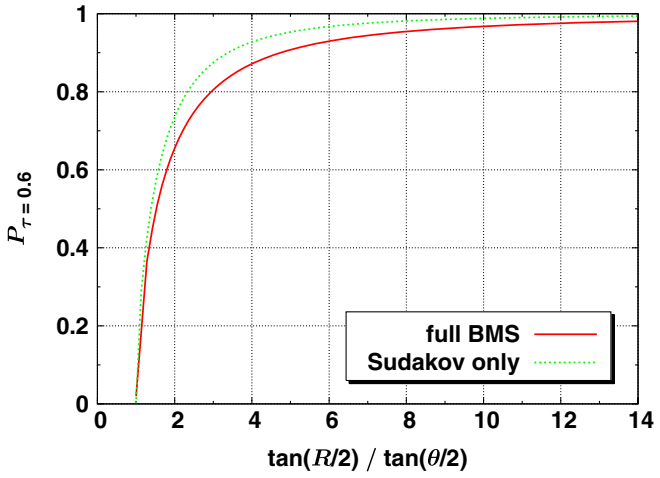

FIG. 8 (color online). Solid red curve: The probability as a function of $\frac{\tan R/2}{\tan\theta/2}$; dotted green curve: Sudakov contribution (33)
.

Let us take, as an illustration, $M = 100$ GeV so that $p_t R/M = 10R$. Then Fig. 8 shows that, if we take $R = 0.4$, with 85% probability energy emitted outside the jet cone is less than 10 GeV. This is only 1% of the jet p_t and is virtually indistinguishable from the underlying event and pileup contributions (assuming that the typical energy scale of the latter is around this value at the LHC). The situation is similar for jets with higher p_t values. Even with $p_t = 4$–5 TeV, τ can reach only up to 0.7 and the function (31) is somewhat decreased overall. However, this is more than compensated by the effect due to the decrease of the $q\bar{q}$ pair opening angle (if M is kept fixed), and again one finds that with very high probability >90%, $E_{\rm out}$ is less than 10 GeV. On the other hand, one can increase τ appreciably if $E_{\rm out}$ is decreased, though 10 GeV might already be a bit too small of a value to choose in high-luminosity measurements at the LHC. The probability distribution of $e_{\rm out} = E_{\rm out}/p_t$ is shown on the right-hand side of Fig. 6 in the previous section, albeit in the fixed coupling case. As a matter of fact, this figure has been obtained for the particular $q\bar{q}$ configuration above ($p_t/M = 10$, $R = 0.4$).

Next we turn to the quark jet. Clearly, energy flow is more efficient in this case. Due again to the QCD coherence, radiation from the qg system with $\theta_{\alpha\beta} \ll 1$ is effectively that from the parent quark. If this quark is created via the $q\bar{q} \to q\bar{q}$ hard scattering with one-gluon exchange, the compensating color is carried by the outgoing jet in the backward direction (Fig. 7, middle). In the $qq \to qq$ case it is carried by one of the incoming partons (Fig. 7, right).[1] We thus consider the two-cone configuration with $\theta_{\rm in} = R$ and take $\theta_{\alpha\beta} = \pi$ and $\pi/2$ in the two cases, respectively. However, solving the BMS equation for the latter case is technically difficult because it involves complicated angular integrations. Rather than doing this, here we give a simple estimate of P_τ by noting that, to lowest order in the small parameter R, the configuration in Fig. 7 (right) is obtained by boosting the back-to-back configuration with $\theta_{\rm in} = \sqrt{2}R$ in a direction orthogonal to the jet axes with velocity $v = 1/\sqrt{2}$. Of course this artificially modifies certain components of the particles' four-momenta up to a factor $\gamma = 1/\sqrt{1 - v^2} = \sqrt{2}$, resulting in a small change in τ mainly via the running of the coupling. (The ratio $p_t/E_{\rm out}$ is less affected by the boost.) But in the present study we ignore this change.

The results are plotted in Fig. 9 as a function of R. In both cases, P_τ is significantly smaller, by a factor of about

[1]There are subleading contributions in N_c where the color flow assignment is interchanged between the two cases.

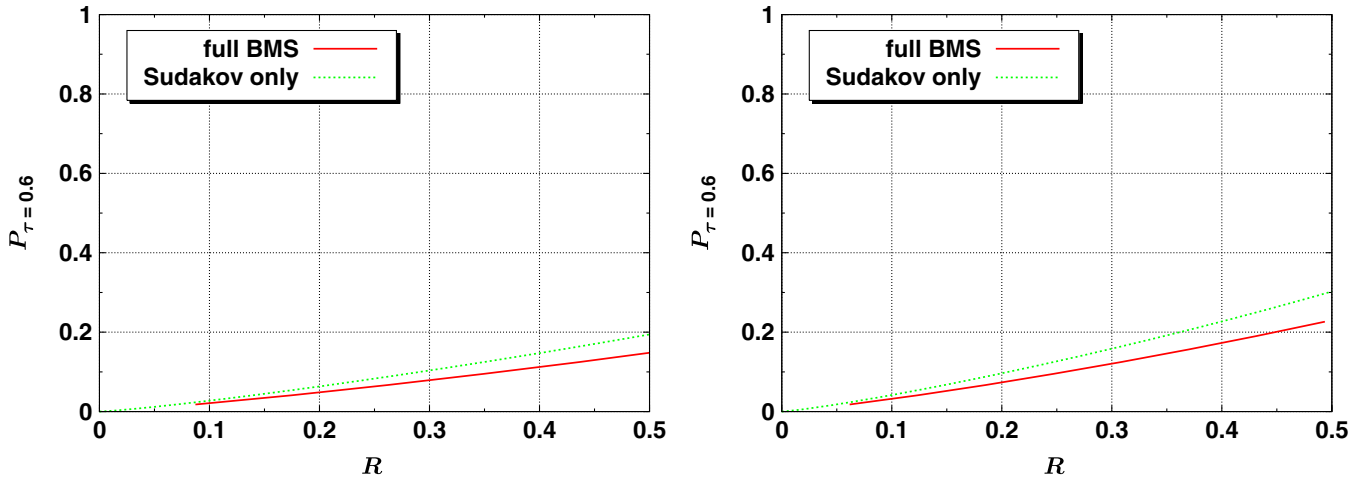

FIG. 9 (color online). Radiation outside the QCD jet as a function of the cone radius. The left- (right-) hand side corresponds to the middle (right) figure in Fig. 7.

5, than in the weak-jet case. With very high probability (80%–90% when $R = 0.4$) the energy radiated outside the jet cone is *greater* than $E_{\rm out} = 10$ GeV, though it is typically smaller than the average value $\langle E_{\rm out}\rangle \sim \alpha_s p_t \gtrsim \mathcal{O}(100)$ GeV as can be inferred from the left-hand side of Fig. 6.

We have thus demonstrated the striking contrast in the amount of energy flow between jets initiated by colorless and colored particles. The fivefold difference in the probability P_τ at first looks like a powerful criterion for the event-by-event identification of jet types. (Note that the average energy is dominated by rare events, so it is not suited for the event-by-event identification.) However, in realistic experiments several other effects are expected to reduce this difference. Most importantly, in the above we have dealt with an idealized situation where there is only one dipole containing the triggered jet, and said nothing about the presence of other dipoles in the process some of which are shown in Fig. 7 in dotted lines. The radiation from these extra dipoles is presumably not much smaller than that from the triggered quark jet, and clearly one has to come up with a method to minimize these backgrounds. A step in the right direction would be to look at the angular region just outside the triggered jet cone where actually most of $E_{\rm out}$ is concentrated.[2] This is briefly explained in Appendix B and will be studied further elsewhere.

V. BFKL DIJET CROSS SECTION WITH PERTURBATIVE GAP SURVIVAL PROBABILITY

Our second example is the production of dijets separated by a large rapidity gap $\Delta\eta$. Such jet-gap-jet events have been reported at the Tevatron some time ago [32,33] and are certainly an interesting channel to study at the LHC given the larger p_t values attainable by forward jets. Two approaches to study jet-gap-jet events in perturbative QCD are commonly used:

(i) In the BFKL approach [34–39], the exchange of the BFKL Pomeron [20,21] in the t channel naturally generates a rapidity gap, which should be the dominant process in the limit of a large gap $\Delta\eta \gg 1$. At the Tevatron, gap events are identified by requiring no activity (above the threshold) in the central rapidity region $|\eta| \le 1$. Yet it seems more natural to define a gap in the true sense of the word, to be the region between the edges of jet cones so that the actual gap size is $\Delta\eta' = \Delta\eta - 2R$, where $\Delta\eta$ is the rapidity difference of dijets. This is desirable also from a theoretical point of view because in this way one can efficiently suppress the contribution from color-octet exchanges so that the signal of the BFKL Pomeron becomes more visible. However, jet cones filled with soft radiation are simply absent at the level of the BFKL cross section, though an event generator may be used to fix this.

(ii) In the factorization approach [5,6,9,10,40], one defines a gap event in terms of energy flow and starts out with the one-gluon exchange. One then dresses the amplitude with soft gluons via the renormalization group with due respect to the constraint in energy flow into the gap region. The BFKL Pomeron does not arise automatically in this approach, rather, it has to be added by hand avoiding double counting [40]. The nonglobal logs are not included, but their effects may be estimated separately [10].

Here we employ the BFKL approach and discuss how to include the effect of soft radiations and of the finite jet cone size. We define gap events in terms of energy flow (as in the factorization approach) and require that the total amount of energy between the edges of jet cones is less than $E_{\rm out}$. Events with a perfect gap would correspond to $E_{\rm out} = 0$, but in order to use perturbation theory one should require $E_{\rm out} \gg \Lambda_{\rm QCD}$. We take, somewhat optimistically, $E_{\rm out} = 1$

[2]Related to this point, we note that the dipole number (not energy) distribution emitted from a boosted $q\bar{q}$ pair can be computed exactly including the nonglobal logarithms [18].

and 2 GeV having in mind low-luminosity measurements.[3]

Specifically, consider pp or $p\bar{p}$ scattering with center-of-mass energy $s = (2E)^2$. We parametrize the momenta of the underlying partonic process $ab \to 12$ as (see, Fig. 10)

$$p_a = (x_a E, 0, 0, x_a E), \tag{34}$$

$$p_b = (x_b E, 0, 0, -x_b E), \tag{35}$$

$$p_1 = (p_t \cosh\eta_1, \vec{p}_t, p_t \sinh\eta_1), \tag{36}$$

$$p_2 = (p_t \cosh\eta_2, -\vec{p}_t, p_t \sinh\eta_2). \tag{37}$$

The relative rapidity of the two jets is $\Delta\eta = \eta_1 - \eta_2$, while the average is $\bar{\eta} = \frac{\eta_1+\eta_2}{2}$.

The cross section in the BFKL approximation is given by ($t \approx -p_t^2$) [34]

$$\frac{d\sigma}{d\Delta\eta d\bar{\eta} dt} = x_a x_b \frac{d\sigma}{dx_a dx_b dt} = x_a x_b f_{\rm eff}(x_a, t) f_{\rm eff}(x_b, t) \frac{d\sigma^{q\bar{q}\to q\bar{q}}}{dt}, \tag{38}$$

where the effective parton distribution is [$C_F = (N_c^2 - 1)/2N_c$]

$$f_{\rm eff}(x, t) = q(x, t) + \bar{q}(x, t) + \frac{N_c^2}{C_F^2} g(x, t), \tag{39}$$

and at the leading logarithmic level,

$$\frac{d\sigma^{q\bar{q}\to q\bar{q}}}{dt} = \frac{4\alpha_s C_F^2}{\pi N_c^2} \frac{1}{t^2} \left(\int d\nu \frac{\nu^2}{(\nu^2 + 1/4)^2} e^{\bar{\alpha}_s \omega(\nu)\Delta\eta} \right)^2, \tag{40}$$

with $\omega(\nu) = 2\,\mathrm{Re}[\psi(1) - \psi(\frac{1}{2} + i\nu)]$. Attempts to include the higher order conformal spins and the next-to-leading logarithmic effects can be found in [37–39].

We now implement the survival probability of the gap against soft radiations. It is well known that the nonforward BFKL amplitude coupled to quarks contains the Sudakov factor

$$\exp\left(-\bar{\alpha}_s \Delta\eta \ln\frac{p_t}{k_t} \right), \tag{41}$$

where $k_t \ll p_t$ represents the loop momentum in the soft region, arising from the exchange of Reggeized gluons in the t channel. This limits emissions into the gap region, but apparently, the amplitude is sensitive to the infrared region. However, as explained in [41], such sensitivity disappears in the Mueller-Tang formula [34]. This renders the partonic cross section (40) truly dominated by short distance physics at the scale $\sqrt{|t|} = p_t$, thereby allowing one to treat it nearly on the same footing as, say, the one-gluon exchange contribution. Once this has been done, however, there arises an additional possibility to fill the gap by soft radiation from color dipoles $(p_a p_1)$ and $(p_b p_2)$. (Since the BFKL exchange is color singlet, color flows as $a \to 1$ and $b \to 2$.) This is not included in the BFKL approximation since the corresponding diagrams are not enhanced by powers of $\Delta\eta$. Still, they are enhanced by powers of $\ln p_t/E_{\rm out}$ and can be taken into account by the survival probability P_τ.

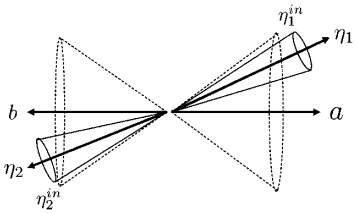

FIG. 10. Radiation from two independent color dipoles.

In the large N_c approximation, radiations from the two dipoles $(p_a p_1)$ and $(p_b p_2)$ are independent. We thus modify (38) as

$$\frac{d\sigma}{d\Delta\eta d\bar{\eta} dt} = x_a x_b \tilde{f}_{\rm eff}(x_a, t) \tilde{f}_{\rm eff}(x_b, t) \times \frac{d\sigma^{q\bar{q}\to q\bar{q}}}{dt} \mathcal{S} P_\tau(\Omega_1, \Omega_a) P_\tau(\Omega_2, \Omega_b), \tag{42}$$

where

$$\tilde{f}_{\rm eff}(x_a, t) = q(x_a, t) + \bar{q}(x_a, t) + \frac{N_c^2}{C_F^2} g(x_a, t) P_\tau(\Omega_1, \Omega_a),$$
$$\tilde{f}_{\rm eff}(x_b, t) = q(x_b, t) + \bar{q}(x_b, t) + \frac{N_c^2}{C_F^2} g(x_b, t) P_\tau(\Omega_2, \Omega_b). \tag{43}$$

$\mathcal{S}$ is the nonperturbative survival probability which concerns the soft interaction among the spectators (the underlying events). It depends only on $\sqrt{s}$ and has been estimated by several groups [42,43]. The presence of an additional factor of P_τ in front of the gluon density in (43) is because at large N_c, a gluon is represented by a double line and radiates like the square of a quark jet.

From (20), one has

$$P_\tau(\Omega_1, \Omega_a) = P_\tau(e^{\eta_1^{\rm in} - \eta_1}) = P_\tau(e^{-R}), \tag{44}$$

where, following our definition of a gap, we choose $\eta_1^{\rm in}$ such that $\eta_1 - \eta_1^{\rm in}$ is always equal to R; see Fig. 10. Similarly, $|\eta_2 - \eta_2^{\rm in}| = R$. Equation (44) means that, once the cone radius is fixed, the perturbative survival probability depends only on p_t (or equivalently, τ) of the

[3]Note that, as already implicit in the previous section, in our definition $E_{\rm out}$ includes only the perturbative radiation from the hard scatterers; that is, the contributions from the underlying event and pileups are subtracted. These are partly taken into account by the nonperturbative survival probability $\mathcal{S}$ introduced later.

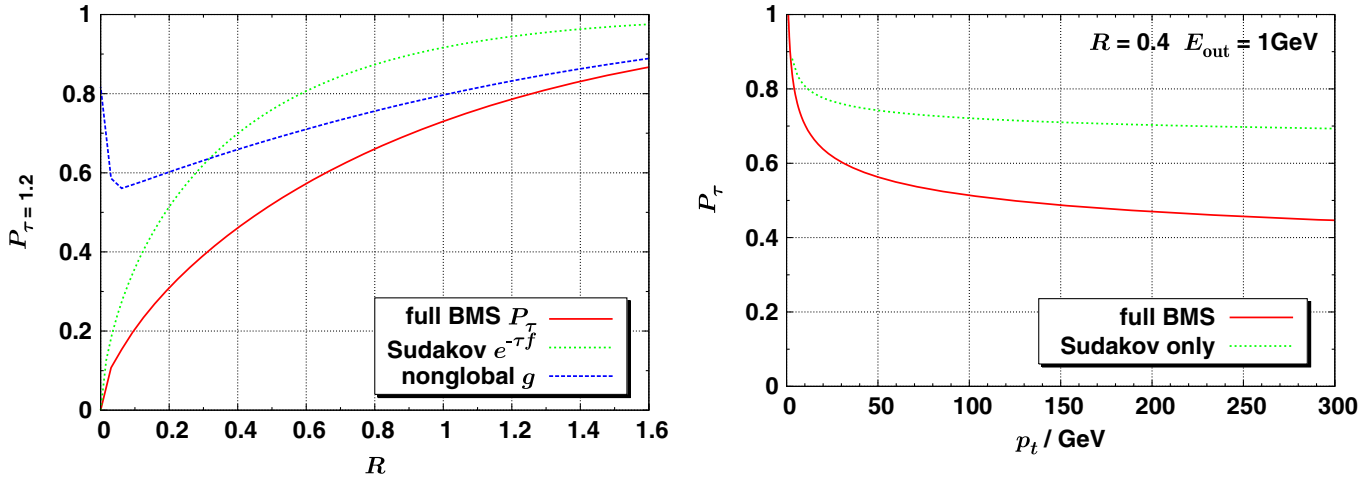

FIG. 11 (color online). Left panel: The survival probability P_τ (solid red line) at $\tau = 1.2$ as a function of the jet cone radius R. The dotted blue line is the Sudakov factor $e^{-\tau f}$ [cf. (22)] and the dotted green line is the nonglobal contribution g. Right panel: The survival probability as a function of p_t for fixed $R = 0.4$.

jets, and not on the rapidity gap $\Delta\eta$ in the present approximation.

On the left-hand side of Fig. 11, we plot (44) as a function of R for fixed $\tau = 1.2$, corresponding to $p_t \sim 300$ GeV and $E_{\rm out} = 1$ GeV in the running coupling case with $\alpha_s(1\ {\rm GeV}) \approx 0.5$. On the right-hand side of Fig. 11, we fix $R = 0.4$ and plot (44) as a function of p_t using the one-loop relation between τ and p_t. The case with $E_{\rm out} = 2$ GeV is shown in Fig. 12. We see that the results depend rather sensitively on the value of $E_{\rm out}$ in the few-GeV region. When $E_{\rm out} = 1$ GeV the nonglobal logarithms are more important than the Sudakov logarithms.

The dependence of P_τ on jet p_t is weak for $p_t > 50$ GeV and is typically $P_\tau \sim 0.5$ when $E_{\rm out} = 1$ GeV. This means that the BFKL cross section gets smaller at least by a factor $P_\tau^2 \sim 0.25$. The gluon-gluon contribution is suppressed by an even smaller factor P_τ^4. On the other hand, by requiring the gap size to grow linearly with the dijet rapidity gap $\Delta\eta' = \Delta\eta - 2R$ and choosing a small $E_{\rm out}$, one can enormously suppress the color-octet contribution. This can be readily inferred from the right branch of Fig. 4. One sees that the typical suppression factor for the color-octet contribution is $P_\tau^2 \sim 0.01$ or less when $\tau = 1.2$. Thus the suppression factor $\sim$0.25 in the color-singlet channel appears to be a small price to pay for a clean test of the BFKL effects. In practice, in order to get the full cross section the above results should be combined with an event generator paying attention to the double counting of the sort discussed in [12].

VI. CONCLUSIONS

In this paper we have presented a detailed numerical study of the BMS equation which describes the dynamics of interjet energy flow at the single-logarithmic level in the large-N_c approximation. In hard scattering processes, en-

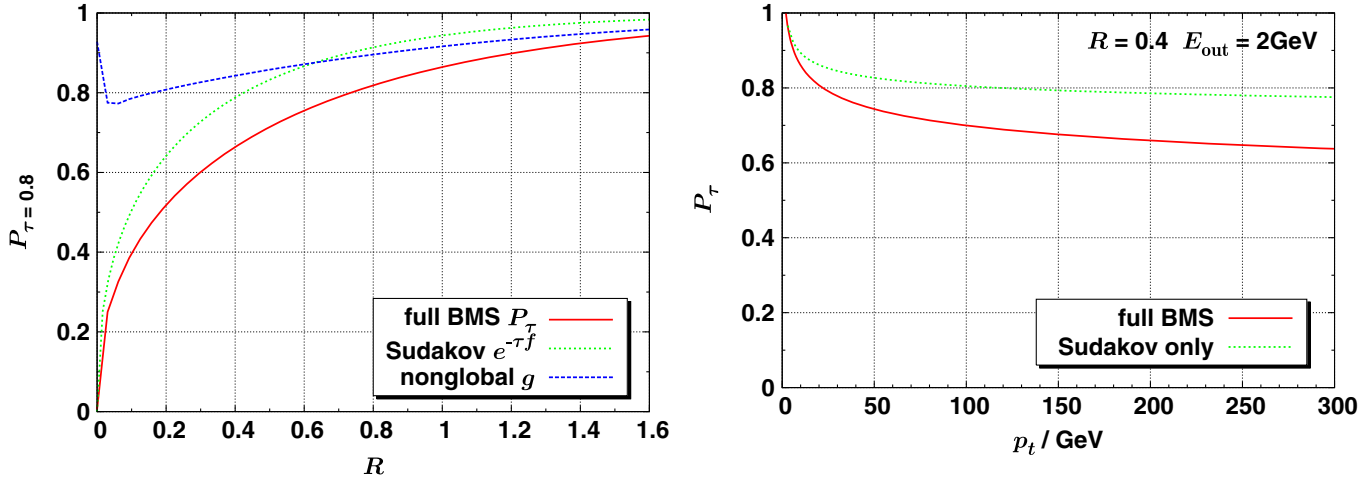

FIG. 12 (color online). Same as Fig. 11 except that $E_{\rm out} = 2$ GeV.

ergy flow is often thought of as an annoying feature which, like the underlying event and the hadronization effect, blurs otherwise clean predictions of perturbative QCD or signatures of new physics [3]. Contrary to this, our main motivation has been to demonstrate the usefulness of energy flow as a primary diagnostic tool to discover interesting physics at collider experiments. We have discussed two examples for this purpose: identifying high-p_t jets of hadronically decaying electroweak bosons among the QCD background, and suppressing the color-octet contribution relative to the BFKL Pomeron contribution in dijet rapidity gap events. Both processes are characterized by the large ratio $p_t/E_{\rm out}$, and we have shown that the consideration of energy flow in terms of the probability P_τ can significantly enhance the signal-to-background ratio. We also suggest that the probability P_τ is better suited to the event-by-event identification of jets than the average energy $\langle E_{\rm out}\rangle$, since the latter does not reflect the property of the majority of events. In the future it remains to integrate the results into the full collision environment to see quantitatively how the nonperturbative effects affect the perturbatively calculated probability P_τ.

ACKNOWLEDGMENTS

We are grateful to Cyrille Marquet and Christophe Royon for many discussions and Shinhong Kim for helpful conversations. Special thanks go to Gavin Salam for reading the manuscript and making valuable suggestions. This work is supported, in part, by Special Coordination Funds for Promoting Science and Technology of the Ministry of Education, Culture, Sports, Science and Technology, of the Japanese Government.

Note added.—While this paper was being finalized, a preprint [44] appeared which also studied energy flow as a tool to identify new particles in a different context.

APPENDIX A: POINCARÉ DISK

The group $\mathrm{SU}(1,1) \cong \mathrm{SO}(1,2)$ is the isometry group of the hyperbolic space H_2 defined by

$$X_0^2 - X_1^2 - X_2^2 = 1. \tag{A1}$$

Via the change of the coordinates

$$X_0 + X_2 = \frac{1}{y}, \qquad x = yX_1, \tag{A2}$$

the space is mapped onto the upper half plane with the squared length element

$$ds^2 = -dX_0^2 + dX_1^2 + dX_2^2 = \frac{d\omega d\bar{\omega}}{y^2}, \tag{A3}$$

where $\omega \equiv x + iy$ and $y \geq 0$. This can be further mapped onto a unit disk via the transformation

$$z = \frac{i\omega + 1}{\omega + i}, \qquad ds^2 = \frac{4dzd\bar{z}}{(1-|z|^2)^2}. \tag{A4}$$

A disk endowed with this metric is known as the Poincaré disk. The invariant distance between two points (the chordal distance) on the Poincaré disk can be immediately derived from that in the H_2 space

$$\begin{aligned} &-(X_0 - X_0')^2 + (X_1 - X_1')^2 + (X_2 - X_2')^2 \\ &= \frac{-4|\omega - \omega'|^2}{(\omega - \bar{\omega})(\omega' - \bar{\omega}')} = \frac{4|z - z'|^2}{(1-|z|^2)(1-|z'|^2)} \\ &\equiv 4d^2(z, z'). \end{aligned} \tag{A5}$$

Using this, one can rewrite the kernel (9) in a manifestly SU(1,1)-invariant form

$$\frac{1}{2\pi}\frac{dz_\gamma d\bar{z}_\gamma}{(1-|z_\gamma|^2)^2}\frac{d^2(z_\alpha, z_\beta)}{d^2(z_\alpha, z_\gamma)d^2(z_\gamma, z_\beta)}. \tag{A6}$$

APPENDIX B: THE AVERAGE ENERGY

In this Appendix, we estimate the rapidity (angular) distribution of $E_{\rm out}$ in the interjet region using (27). As already noted, strictly speaking this goes beyond the validity range of the soft approximation. But nevertheless we wish to record the result here for possible future applications.

Let us begin with a dipole formed by the incoming partons as shown by dotted lines in the left and middle figures of Fig. 7. Since the τ integral in (27) is dominated by the small-τ region, one may approximate P_τ by its Sudakov part. Actually, one can go one step further to include the first correction from the nonglobal logarithm [8,13]. This gives

$$P_\tau(\theta_{\rm in}) \approx e^{-\tau R_0 - \tau^2 R_1}, \tag{B1}$$

where

$$\begin{aligned} R_0 &= 2\ln\cot\frac{\theta_{\rm in}}{2} = 2\eta_{\rm in}, \\ R_1 &= \frac{\pi^2}{12} - \frac{\mathrm{Li}_2\tan^4\frac{\theta_{\rm in}}{2}}{2} = \frac{\pi^2}{12} - \frac{\mathrm{Li}_2 e^{-4\eta_{\rm in}}}{2}. \end{aligned} \tag{B2}$$

(Li_2 is the dilogarithm function.) Therefore,

$$\begin{aligned} \frac{\langle E_{\rm out}\rangle}{p_t} &= 1 - \frac{1}{\bar{\alpha}_s}\int_0^\infty d\tau e^{-[(1/\bar{\alpha}_s)+R_0]\tau - R_1\tau^2} \\ &= 1 - \frac{\sqrt{\pi}}{2\bar{\alpha}_s\sqrt{R_1}} e^{[(1/\bar{\alpha}_s)+R_0]^2/(4R_1)} \mathrm{Erfc}\left(\frac{\frac{1}{\bar{\alpha}_s} + R_0}{2\sqrt{R_1}}\right), \end{aligned} \tag{B3}$$

where Erfc is the complementary error function. Let us then introduce a differential distribution

$$\langle E_{\rm out}\rangle = \int_{-\eta_{\rm in}}^{\eta_{\rm in}} d\eta \left\langle \frac{dE_{\rm out}}{d\eta}\right\rangle = 2\int_0^{\eta_{\rm in}} d\eta \left\langle \frac{dE_{\rm out}}{d\eta}\right\rangle, \tag{B4}$$

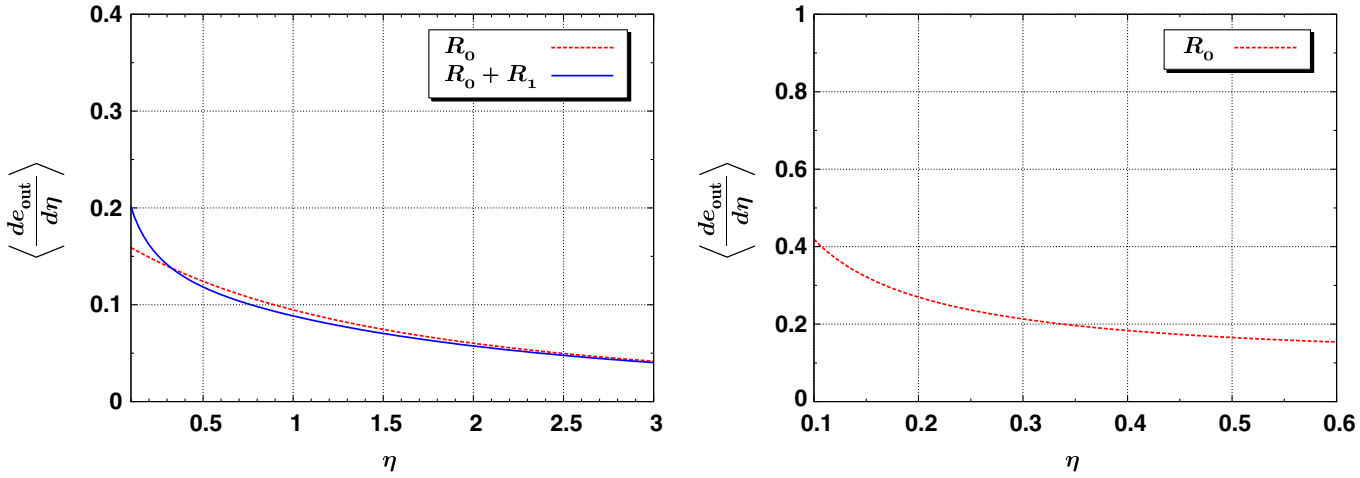

FIG. 13 (color online). Left panel: The rapidity distribution of $E_{\rm out}$ emitted from the dipole formed by incoming partons. The region $\eta < p_t/M = 0.1$ is excluded. Right panel: The rapidity distribution of $E_{\rm out}$ near the quark jet.

such that

$$\left\langle \frac{dE_{\rm out}}{d\eta} \right\rangle = \frac{1}{2} \frac{\partial \langle E_{\rm out} \rangle}{\partial \eta_{\rm in}} \bigg|_{\eta_{\rm in}=\eta}. \tag{B5}$$

Equation (B5) is plotted on the left-hand side of Fig. 13 with or without the R_1 term. The distribution is flat to lowest order in α_s, but after the exponentiation it slowly varies with η. Note that $E_{\rm out}$ in this case should be understood as the total transverse momentum. To get the energy distribution one has to multiply the result by the factor $1/\sin\theta = \cosh\eta$.

Next we consider the back-to-back dipole including the outgoing quark jet, Fig. 7 (middle). This is basically the same configuration as above, but now we have to set the rapidity of the jet to be zero (rather than infinity). Then it is convenient to begin with the angular variable and approximate $\theta_{\rm in} \approx R$ for small R. One finds, omitting the R_1 term,

$$\frac{\langle E_{\rm out} \rangle}{p_t} = \int_R^{\pi - R} \left\langle \frac{de_{\rm out}}{d\theta} \right\rangle d\theta = \frac{2\bar{\alpha}_s \ln\cot\frac{R}{2}}{1 + 2\bar{\alpha}_s \ln\cot\frac{R}{2}}$$
$$\approx 2\bar{\alpha}_s \ln\frac{2}{R} + \mathcal{O}(\alpha_s^2). \tag{B6}$$

If one takes only the first term in the α_s expansion, there is a logarithmic divergence as $R \to 0$. This was discussed in [24], but the coefficient here is different because we have included only the term in the splitting function which is singular in the soft limit. On the other hand, the all-order expression in (B6) is finite as $R \to 0$, and may be regarded as a partial resummation of the logarithms $(\alpha_s \ln R)^n$. The resulting rapidity distribution $\langle de_{\rm out}/d\eta \rangle \approx \langle de_{\rm out}/d\theta \rangle$ is plotted on the right-hand side of Fig. 13. Compared with the left-hand side of Fig. 13, one sees that the shape is similar, but the magnitude is bigger by a factor of 2 in the same η range around midrapidity.

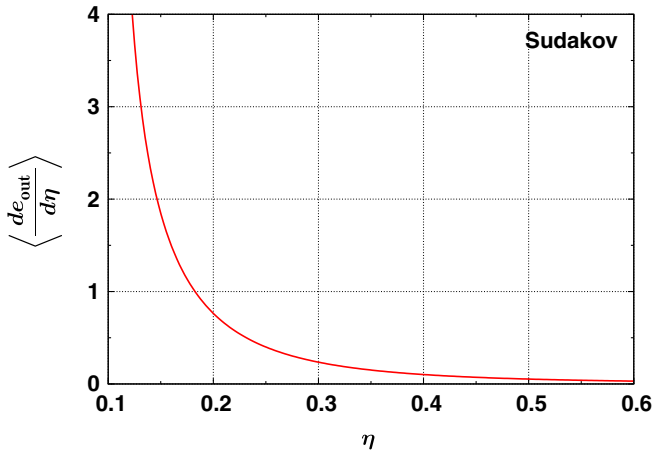

FIG. 14 (color online). The rapidity distribution of $E_{\rm out}$ near a weak boson jet.

Finally, Fig. 14 shows the rapidity (angular) distribution of $E_{\rm out}$ emitted from the weak boson jet with $p_t/M = 10$ calculated from (33). The distribution is very strongly peaked at small η in striking contrast with the previous two cases. This is another way of seeing the difficulty to lose energy for a weak boson jet; see, also, [26].

[1] S. D. Ellis, J. Huston, K. Hatakeyama, P. Loch, and M. Tonnesmann, Prog. Part. Nucl. Phys. **60**, 484 (2008).
[2] G. P. Salam, arXiv:0906.1833.
[3] A. Bhatti *et al.*, Nucl. Instrum. Methods Phys. Res., Sect.

A 566, 375 (2006).
[4] N. Kidonakis, G. Oderda, and G. Sterman, Nucl. Phys. **B531**, 365 (1998).
[5] G. Oderda and G. Sterman, Phys. Rev. Lett. **81**, 3591 (1998).
[6] J. Forshaw, J. Keates, and S. Marzani, J. High Energy Phys. 07 (2009) 023.
[7] M. Dasgupta and G. P. Salam, Phys. Lett. B **512**, 323 (2001).
[8] M. Dasgupta and G. P. Salam, J. High Energy Phys. 03 (2002) 017.
[9] R. B. Appleby and M. H. Seymour, J. High Energy Phys. 12 (2002) 063.
[10] R. B. Appleby and M. H. Seymour, J. High Energy Phys. 09 (2003) 056.
[11] Y. Delenda, R. Appleby, M. Dasgupta, and A. Banfi, J. High Energy Phys. 12 (2006) 044.
[12] A. Banfi, G. Corcella, and M. Dasgupta, J. High Energy Phys. 03 (2007) 050.
[13] A. Banfi, G. Marchesini, and G. Smye, J. High Energy Phys. 08 (2002) 006.
[14] G. Marchesini and A. H. Mueller, Phys. Lett. B **575**, 37 (2003).
[15] G. Marchesini and E. Onofri, J. High Energy Phys. 07 (2004) 031.
[16] H. Weigert, Nucl. Phys. **B685**, 321 (2004).
[17] Y. Hatta, J. High Energy Phys. 11 (2008) 057.
[18] E. Avsar, Y. Hatta, and T. Matsuo, J. High Energy Phys. 06 (2009) 011.
[19] K. Agashe, S. Gopalakrishna, T. Han, G.-Y. Huang, and A. Soni, arXiv:0810.1497.
[20] E. A. Kuraev, L. N. Lipatov, and V. S. Fadin, Sov. Phys. JETP **45**, 199 (1977).
[21] I. I. Balitsky and L. N. Lipatov, Sov. J. Nucl. Phys. **28**, 822 (1978).
[22] I. Balitsky, Nucl. Phys. **B463**, 99 (1996).
[23] Y. V. Kovchegov, Phys. Rev. D **60**, 034008 (1999).
[24] M. Dasgupta, L. Magnea, and G. P. Salam, J. High Energy Phys. 02 (2008) 055.
[25] J. M. Butterworth, B. E. Cox, and J. R. Forshaw, Phys. Rev. D **65**, 096014 (2002).
[26] L. G. Almeida *et al.*, Phys. Rev. D **79**, 074017 (2009).
[27] J. M. Butterworth, A. R. Davison, M. Rubin, and G. P. Salam, Phys. Rev. Lett. **100**, 242001 (2008).
[28] J. Thaler and L.-T. Wang, J. High Energy Phys. 07 (2008) 092.
[29] D. E. Kaplan, K. Rehermann, M. D. Schwartz, and B. Tweedie, Phys. Rev. Lett. **101**, 142001 (2008).
[30] L. G. Almeida, S. J. Lee, G. Perez, I. Sung, and J. Virzi, Phys. Rev. D **79**, 074012 (2009).
[31] S. D. Ellis, C. K. Vermilion, and J. R. Walsh, Phys. Rev. D **80**, 051501 (2009).
[32] B. Abbott *et al.* (D0 Collaboration), Phys. Lett. B **440**, 189 (1998).
[33] F. Abe *et al.* (CDF Collaboration), Phys. Rev. Lett. **80**, 1156 (1998).
[34] A. H. Mueller and W.-K. Tang, Phys. Lett. B **284**, 123 (1992).
[35] V. Del Duca and W.-K. Tang, Phys. Lett. B **312**, 225 (1993).
[36] B. Cox, J. R. Forshaw, and L. Lonnblad, J. High Energy Phys. 10 (1999) 023.
[37] R. Enberg, G. Ingelman, and L. Motyka, Phys. Lett. B **524**, 273 (2002).
[38] L. Motyka, A. D. Martin, and M. G. Ryskin, Phys. Lett. B **524**, 107 (2002).
[39] F. Chevallier, O. Kepka, C. Marquet, and C. Royon, Phys. Rev. D **79**, 094019 (2009).
[40] J. R. Forshaw, A. Kyrieleis, and M. H. Seymour, J. High Energy Phys. 06 (2005) 034.
[41] J. Bartels *et al.*, Phys. Lett. B **348**, 589 (1995).
[42] E. Gotsman, E. Levin, and U. Maor, Phys. Lett. B **438**, 229 (1998).
[43] A. B. Kaidalov, V. A. Khoze, A. D. Martin, and M. G. Ryskin, Eur. Phys. J. C **21**, 521 (2001).
[44] I. Sung, arXiv:0908.3688.